PHYSICAL REVIEW D **92,** 123537 (2015)

Early dark energy and its interaction with dark matter

Bo-Yu Pu, Xiao-Dong Xu, and Bin Wang
IFSA Collaborative Innovation Center, Department of Physics and Astronomy, Shanghai Jiao Tong University, Shanghai 200240, China

Elcio Abdalla
Instituto de Fisica, Universidade de Sao Paulo, CEP 05315-970 Sao Paulo, Brazil
(Received 26 August 2015; published 29 December 2015)

We study a class of early dark energy models which has a substantial amount of dark energy in the early epoch of the Universe. We examine the impact of the early dark energy fluctuations on the growth of structure and the cosmic microwave background power spectrum in the linear approximation. Furthermore, we investigate the influence of the interaction between the early dark energy and the dark matter and its effect on the structure growth and cosmic microwave background. We finally constrain the early dark energy model parameters and the coupling between dark sectors by confronting different observations.

DOI: 10.1103/PhysRevD.92.123537 PACS numbers: 98.80.-k

I. INTRODUCTION

From astronomical observations, it is convincing that our Universe is undergoing accelerated expansion. The driving force of this acceleration is dark energy (DE), which composes roughly 70% of the total energy budget of our Universe. The physical nature of DE, together with its origin and time evolution, is one of the most enigmatic puzzles in modern cosmology. The simplest explanation of DE is the cosmological constant with the equation of state (EoS) $w = -1$. Although the cosmological constant fits well to current observational data, it suffers serious theoretical problems. One is the cosmological constant problem, the fact that the quantum field theory prediction for the value of Λ is about a hundred orders of magnitude larger than the observation [1]. Another problem, more closely related to the cosmological evolution itself, is the coincidence problem, namely, why, since it is a constant, the Λ value becomes important for the evolution of the Universe just at the present moment [2]. Besides the cosmological constant, there are other alternative explanations of DE. But so far, the focus has been on the EoS of DE and in particular on its current value w_0.

It is rather the amount of DE, Ω_{de}, than the EoS that influences the evolution of our Universe. In this spirit, an interesting subclass of DE models involving a non-negligible DE contribution at early times has been proposed. These models are called early dark energy (EDE) and have been extensively studied recently. EDE models can potentially alleviate the coincidence problem. Furthermore, they can influence the cosmic microwave background [3–9], big bang nucleosynthesis [10], and large-scale structure formation [11–17]. For now, it would be fair to say that there are no strong observational constraints on the EDE models, and it is especially difficult to discriminate EDE models which have $w = -1$ at present from the ΛCDM model.

In this paper, we will focus on a specific EDE model, which is similar to that originally introduced by Wetterich [18] and further examined in Ref. [14]. This model is characterized by a low but nonvanishing DE density at early times with the EoS varying with time in the form

$$w(z) = \frac{w_0}{1 + b\ln(1+z)^2}, \qquad b = -\frac{3w_0}{\ln(\frac{1-\Omega_{de,e}}{\Omega_{de,e}}) + \ln(\frac{1-\Omega_{m,0}}{\Omega_{m,0}})}, \tag{1}$$

where w_0 and $\Omega_{de,0} = 1 - \Omega_{m,0}$ represent the present-day EoS and amount of DE, respectively, while $\Omega_{de,e}$ gives the average energy density parameter at early times. The parameterization (1) has been constrained by type Ia supernova observations including samples at $z > 1.25$ [19,20]. The impact of this EDE cosmology on galaxy properties has been studied by coupling high-resolution numerical simulations with semianalytic modeling of galaxy formation and evolution [13]. The available results highlight that such an EDE model leads to important modifications in the galaxy properties with respect to a standard ΛCDM universe.

We use this dynamical EDE parametrization to further discuss the influence of this specific model on the cosmic microwave background radiation (CMB) and compare it with the ΛCDM prediction. For dynamical DE models, in contrast with ΛCDM, they possess DE fluctuations. In the linear regime, these fluctuations for usual DE models, for example, quintessence, are usually several orders of magnitude smaller than that of dark matter (DM) so that DE fluctuations are usually neglected in studies of CMB and structure formations in the linear approximation. It would be interesting to examine the presence of the EDE fluctuation and its impact on the DM perturbations and CMB and compare this with the usual assumption of nearly

homogeneous EDE and ΛCDM models. This can help to distinguish between homogeneous and inhomogeneous EDE models and also disclose the difference from the ΛCDM model. Moreover, we will attempt to constrain this EDE model using current data. In Ref. [9], one different type of EDE model was constrained by using observational data at high redshift including the WMAP five year data for CMB, but in that study, the authors have not compared different effects brought by the inhomogeneous and homogeneous EDE.

It is clear that DM and DE are the two main components of our Universe, which compose almost 95% of the total Universe. It is a special assumption that these two biggest components exist independently in the Universe. A more natural understanding, in the framework of field theory, is to consider that there is some kind of interaction between them. It has been shown that the interaction between DM and DE is allowed by astronomical observations and can help to alleviate the coincidence problem; see, for example, Refs. [21–25] and references therein. It would be of great interest to extend the previous studies to the interaction between EDE and DM. With the non-negligible DE energy density at high redshift, the interaction between dark sectors will start to play the role earlier. To investigate the influence of the interaction between EDE and DM on the structure growth and CMB signals is the second objective of this paper.

The outline of the paper is the following. In the next section, we will first present the background evolution of the EDE model and discuss the influence of the interaction between dark sectors on the background dynamics. And then we will study evolutions of linear perturbations of a system with EDE and pressureless matter and calculate the growth of the structure. We will examine the effect of the interaction between EDE and DM on the linear perturbations. Section III is devoted to the study of the CMB power spectrum. In Sec. IV. we will present the constraint of the EDE model from fittings to current observational data, and in the last section, we will present our conclusions.

II. ANALYTICAL FORMALISM

In this paper, we investigate the EDE model presented in (1), in which there is a low but nonvanishing DE density at early times. We modified the CAMB code to examine the influences of the EDE on the background evolution, linear perturbation, and CMB power spectrum by performing analysis for two models, EDE1 and EDE2, which have $w_0 = -0.93$, $\Omega_{de,e} = 2\times10^{-4}(b = 0.29, \Omega_{m,0} = 0.25)$ and $w_0 = -1.07$, $\Omega_{de,e} = 2\times10^{-4}(b = 0.33, \Omega_{m,0} = 0.25)$, respectively.

Figure 1 shows the evolutions of the EoS in the EDE models that we examine in this work. The amount of DE at early times is nonvanishing, and EDE models approach the cosmological constant scenario at recent times. The EDE1 model has an EoS always above -1, while the EDE2 EoS can cross -1 and stay below -1 at present.

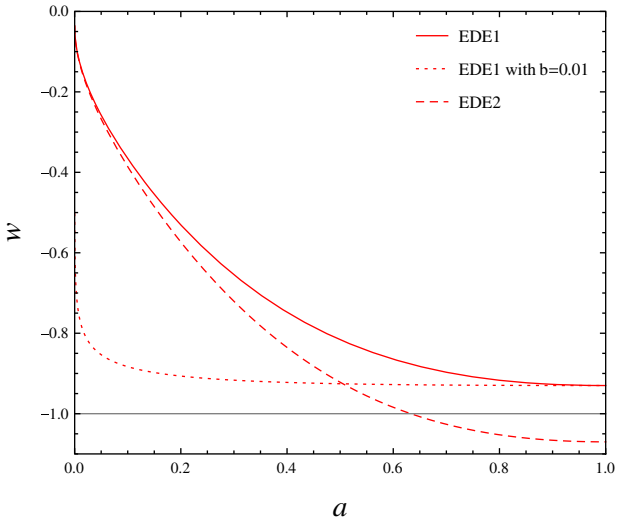

FIG. 1 (color online). EoS of two EDE models. The dotted line refers to the EDE1 with b = 0.01.

In the spatially flat Friedmann-Robertson-Walker universe, the evolutions of the energy densities of DE and DM in the background spacetime are governed by

$$\rho'_{dm} + 3\mathcal{H}\rho_{dm} = aQ_{dm}$$
$$\rho'_{de} + 3\mathcal{H}(1+w)\rho_{de} = aQ_{de}, \tag{2}$$

where H is the Hubble constant and $\mathcal{H} = aH$ with a the scale factor of the universe. Q_α indicates the interaction between dark sectors, where the subscript α refers to dm or de, respectively. We show the evolution of the DE fractional energy density when there is no interaction between DE and DM in Fig. 2. In the left panel of Fig. 2, we compare the Ω_{de} for EDE1 with constant EoS DE and cosmological constant. We can see that for the model EDE1 DE started to have a significant ratio in the budget of the universe earlier, which helped to alleviate the coincidence problem. We also compare the evolution of Ω_{de} for different EDE models with that of the cosmological constant in the right panel of Fig. 2. The evolution of Ω_{de} shows that the model EDE1 is favorable to ease the coincidence problem. To see more clearly, we present the behavior on the ratio ρ_{dm}/ρ_{de} in Fig. 3. It is easy to see that the ratio for EDE1 is smaller at early times. This shows that the ratio for EDE1 evolves more slowly so that it has a longer period for the energy densities of EDE1 and DM to be comparable, in the spirit of alleviating the coincidence problem.

Since we know the nature of neither DM nor DE, it is hard to describe the interaction between them, although there have been some attempts on this task [26–29]. Our study on the interaction between dark sectors will concentrate on the phenomenological descriptions. We assume

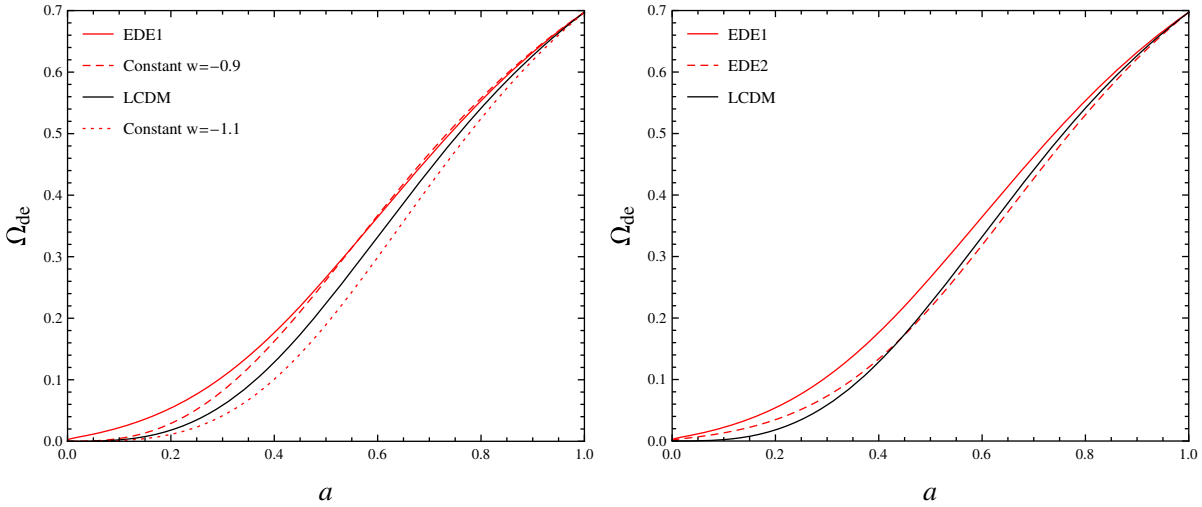

FIG. 2 (color online). The evolutions of DE fractional energy densities for different DE models when there is no interaction between dark sectors.

there is energy flow due to the interaction between dark sectors where the coupling vector is defined in the form $Q^\nu = (\frac{Q}{a}, 0, 0, 0)^T$ [23], and Q takes the phenomenological form $Q = 3\lambda_1 H\rho_{dm}$ or $Q = 3\lambda_2 H\rho_{de}$, where λ_1 and λ_2 refer to the strengths of the respective couplings.

We plot the evolution of the DE fractional energy density in Fig. 4. In the left panel, we choose the interaction as being proportional to the energy density of DM. For the EDE model, with the positive coupling proportional to the DM energy density ($\lambda_1 > 0$), the influence of DE in the universe evolution appeared much earlier. The positive coupling, in our notation, indicates that energy flows from DE to DM [21–25]. For the same amount of DE today, with the positive coupling, it implies that DE density was higher in the past. The coupling strength λ_1 cannot be chosen negative, since the negative λ_1 will lead to the negative DE fractional energy density Ω_{de} at early time of the universe, as is shown in the middle panel of Fig. 4, which is certainly unphysical. In the right panel of Fig. 4, we show the case where the interaction is proportional to the DE density. We see that for the EDE1 model with positive coupling ($\lambda_2 > 0$) if the EDE model has the same amount of DE as that of the ΛCDM model to drive the acceleration of the Universe today, it must have more EDE at high redshift, which we also argued to have consequences related to DM phenomenology in accordance with the results of BOSS [30]. But compared to the left panel, the influence of the coupling is weaker in the right panel. This is easy to understand, because in the right panel, the interaction is proportional to DE energy density, which was much lower than that of DM at early times in the universe.

Besides the background dynamics, we can extend the study to the linear relativistic evolution of the system of DE and DM. The gauge-invariant linear perturbation equations of the system were derived in Refs. [23,31–33]. Using the phenomenological form of the energy transfer between dark sectors defined above, the equations yield

$$
\begin{aligned}
D'_{dm} &= -kU_{dm} + 3\mathcal{H}\Psi(\lambda_1 + \lambda_2/r) - 3(\lambda_1 + \lambda_2/r)\Phi' + 3\mathcal{H}\lambda_2(D_{de} - D_{dm})/r,\\
U'_{dm} &= -\mathcal{H}U_{dm} + k\Psi - 3\mathcal{H}(\lambda_1 + \lambda_2/r)U_{dm};\\
D'_{de} &= -3\mathcal{H}(C_e^2 - w)D_{de} + \{3w' - 9\mathcal{H}(w - C_e^2)(\lambda_1 r + \lambda_2 + 1 + w)\}\Phi,\\
&\quad - 9\mathcal{H}^2(C_e^2 - C_a^2)\frac{U_{de}}{k} + 3(\lambda_1 r + \lambda_2)\Phi' - 3\Psi\mathcal{H}(\lambda_1 r + \lambda_2) + 3\mathcal{H}\lambda_1 r(D_{de} - D_{dm})\\
&\quad - 9\mathcal{H}^2(C_e^2 - C_a^2)(\lambda_1 r + \lambda_2)\frac{U_{de}}{(1+w)k} - kU_{de},\\
U'_{de} &= -\mathcal{H}(1 - 3w)U_{de} - 3kC_e^2(\lambda_1 r + \lambda_2 + 1 + w)\Phi + 3\mathcal{H}(C_e^2 - C_a^2)(\lambda_1 r + \lambda_2)\frac{U_{de}}{(1+w)}\\
&\quad + 3(C_e^2 - C_a^2)\mathcal{H}U_{de} + kC_e^2 D_{de} + (1+w)k\Psi + 3\mathcal{H}(\lambda_1 r + \lambda_2)U_{de},
\end{aligned}
\tag{3}
$$

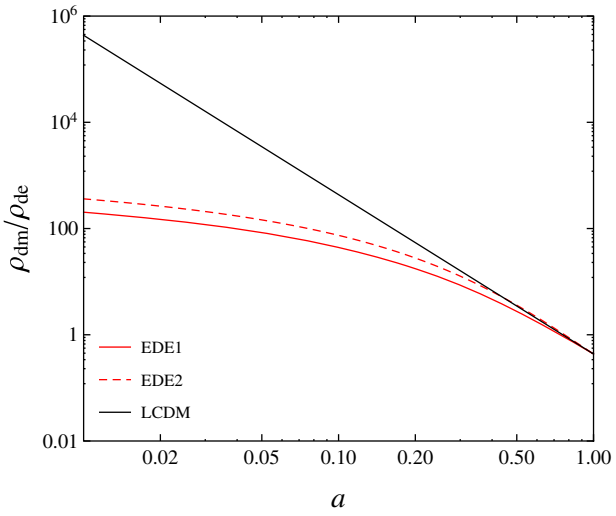

FIG. 3 (color online). The ratio of DM densities to DE densities for different DE models when there is no interaction between dark sectors.

where Ψ, Φ are gauge invariant gravitational potentials, $D_\alpha = \delta_\alpha - \frac{\rho'_\alpha}{\rho\mathcal{H}}\Phi$ is the gauge-invariant density contrast, $U_\alpha = (1+w_\alpha)V_\alpha$, V_α is the gauge-invariant peculiar velocity, and $r \equiv \rho_{dm}/\rho_{de}$ is the energy density ratio of DM and DE. C_a is the adiabatic sound speed of DE, and C_e is the effective sound speed of DE, which we will set to be 1 in this work. Having these perturbation equations, we are in a position to discuss the evolutions of DE and DM density perturbations.

Assuming $\lambda_1 = \lambda_2 = 0$ in (3), we display the evolution of the DE perturbation in the left panel of Fig. 5. In contrast to the DE models with constant EoS, which always have very small DE fluctuations, we see that, although the fluctuation of EDE decays to zero as its EoS approaches the cosmological constant, at early times, when EDE started to play a significant role, its fluctuation was not too small. It would be interesting to investigate how the EDE perturbation influences the growth of DM perturbations. We display the result in Fig. 6(a), where we show the evolution of the DM density perturbation in different DE models. It is clear that the earlier presence of non-negligible

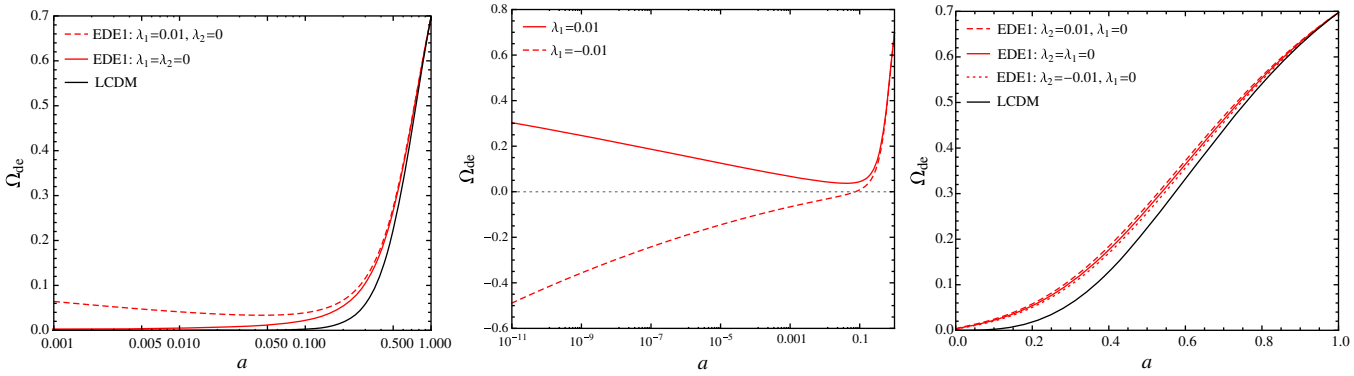

FIG. 4 (color online). The evolutions of DE fractional densities when there is an interaction between dark sectors.

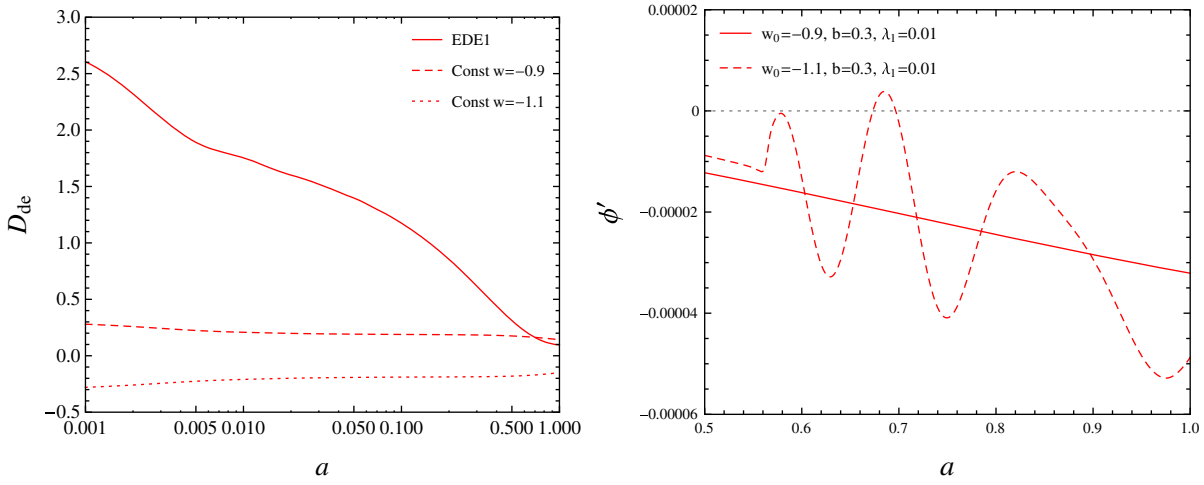

FIG. 5 (color online). Left panel: The evolutions of DE perturbations. Right panel: The time derivative of the gravitational potential.

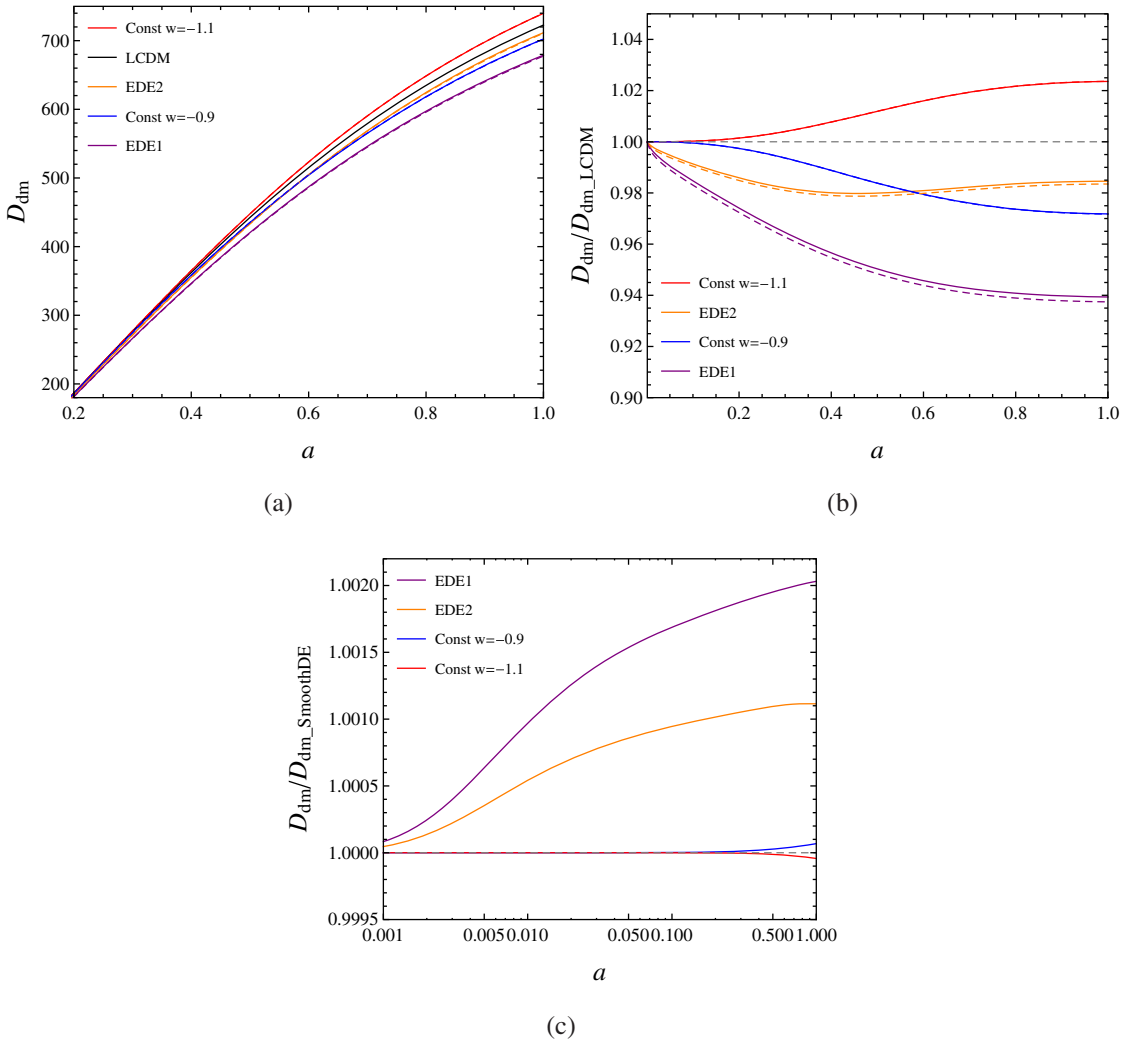

FIG. 6 (color online). (a) The evolutions of DM perturbations. (b) The comparison of DM perturbation evolutions with those of the ΛCDM model. (c) The comparison of DM perturbation evolutions with and without DE perturbations. The solid lines refer to models taking into account DE perturbations. The dashed lines refer to the models assuming homogenous DE.

DE fractional density in the background suppresses the growth in the DM perturbation. To see more closely, we have compared the evolution of the DM perturbation to the standard ΛCDM model in Fig. 6(b). DM perturbations were suppressed compared with the ΛCDM model if DE is described by EDE2, constant $w = -0.9$, and EDE1. The only exception is when DE has a constant EoS $w = -1.1$. The difference in the structure growth from that of the ΛCDM model can be mainly attributed to the differences in the background DE fractional energy density from the standard ΛCDM model. The suppression of the growth of perturbations was caused by the excessive amount of DE compared to that in the ΛCDM model at the early epoch, which hindered gravitational attraction and weakened the growth of DM perturbations. For the EDE models, especially EDE1, the further excess of Ω_{de} at early times suppresses the structure growth even more. The solid lines indicate the models having DE perturbation, while the dashed lines are for the homogeneous DE models where the DE perturbations are neglected. For the DE models with a constant EoS, the difference of effects on the DM perturbations caused by homogeneous and inhomogeneous DE is negligible. This can be further seen in Fig. 6(c). But for EDE models, we clearly see the differences between the solid and dashed lines for the inhomogeneous and homogeneous DE. Figure 6(c) shows this property much more clearly. This is understandable because for the DE with constant EoS the DE perturbation itself is tiny. However, for the EDE models, we clearly see that, different from the homogeneous DE model, the DE perturbations do have an impact on DM perturbations.

Considering the interaction between dark sectors, the situation becomes more complicated. To clearly see the influence of the interaction in dark sectors on the linear perturbations, we concentrate on the DE model EDE1, because in EDE1 the DE EoS is always greater than −1.

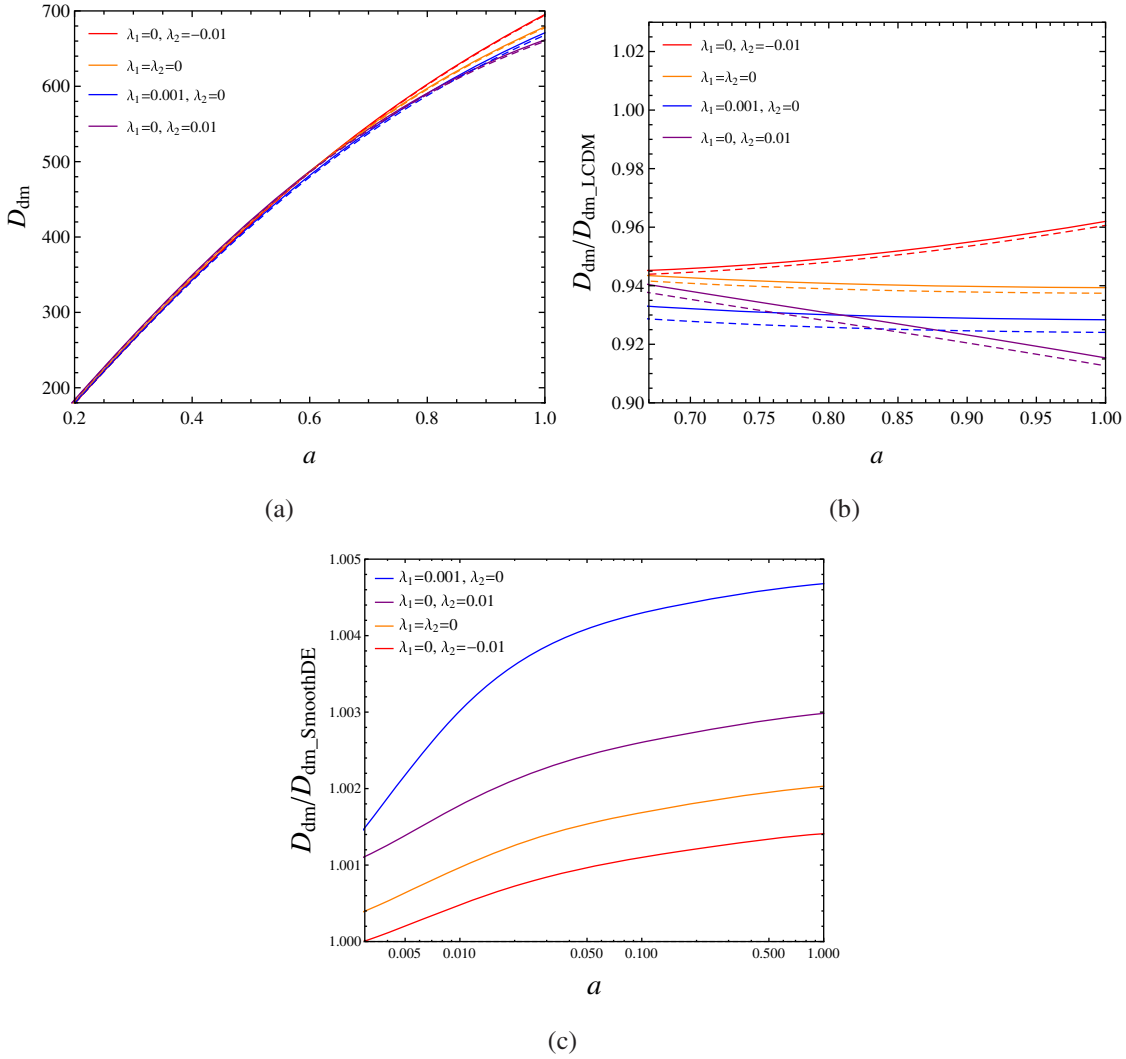

FIG. 7 (color online). (a) DM perturbations when EDE interacts with DM. (b) The comparison of DM perturbation evolutions with that of the ΛCDM model. (c) The comparison of DM perturbation evolutions between models with and without DE perturbations. The solid lines refer to models taking into account DE perturbations. The dashed lines refer to the models assuming homogenous DE.

$1 + w$ has to be positive in order to avoid oscillation in the time derivative of the gravitational potential on large scales if the interaction between dark sectors is proportional to the energy density of DM, which is inconsistent with observations, as shown in the right panel of Fig. 5. In Fig. 7(a), we see that at the present moment for the model with energy decay from EDE to DM the DM perturbation is smaller, which is different from the case with energy decay in the opposite direction. This is easy to understand, because for the positive coupling the background, Ω_{de} was bigger in the past, which hindered the structure growth. In Fig. 7(b), we present the comparison of the DM perturbations between the interacting EDE model and the ΛCDM model. It is clear that, comparing with the ΛCDM model, EDE interacting with DM leads to smaller DM perturbations. For the interaction between dark sectors proportional to the energy density of DM, the effect of the interaction showed up earlier. A positive λ_1 implies more DE in the past, bringing further suppression in the DM perturbations at the early time. For the interaction between dark sectors proportional to the density of DE, the effect showed up later when DE started to dominate. A positive λ_2 indicates the energy flow from EDE to DM, which implies that there was more DE in the past, preventing the DM perturbations further. This explains why the line in Fig. 7(b) with positive λ_2 is lower. For negative λ_2, energy flows from DM to DE. To have the observed amount of DM now, there must have been more DM in the past, which implies faster growth of DM perturbation. Since this effect of the interaction started to appear when DE became important and became more influential in the era of accelerated expansion, lines corresponding to positive and negative λ_2 in Fig. 7(b) deviate from the noninteracting case late in the history of the Universe. The solid and dashed lines in Fig. 7(b) refer to inhomogeneous and homogeneous DE, respectively. We see that DM perturbations differ by

including the DE perturbations or not. This can be seen much more clearly in Fig. 7(c). Comparing with Fig. 6(c), we see that when energy flows from DE to DM, the difference in the DM perturbations caused by the inhomogeneous DE and homogeneous DE is enlarged. Also from Fig. 7(c), we see that the difference in the DM perturbations between inhomogeneous and homogeneous DE is more sensitive to the coupling if it is proportional to the energy density of DM.

III. CMB POWER SPECTRUM

Once we have the understanding of the linear perturbations for DM and DE, we can proceed to study the effects of DE models on CMB. On large scales, the CMB power spectrum is composed of the ordinary Sachs-Wolfe (SW) effect and the Integrated SW (ISW) effect. The SW effect indicates the photons' initial condition when they left the last scattering surface, while the ISW effect is the contribution due to the change of the gravitational potential when photons pass through the universe on their way to Earth. The gauge-invariant gravitational potential in the absence of anisotropic stress can be given by the Poisson equation $k^2\Phi = -4\pi G a^2 \delta\rho$. Its derivative in the DM plus DE universe, which is the source term for the ISW contribution, is given by $k^2\Phi' = -4\pi G \frac{\partial}{\partial\eta}[a^2(\delta\rho_{dm} + \delta\rho_{de})]$. Thus, the large-scale CMB power spectrum depends on the evolution of the density perturbations of DE and DM. However, it should be noted that the ISW effect is complicated. Besides density perturbations in DM and DE, other cosmological parameters such as the EoS of DE, background energy densities, H_0, etc., also influence it. Only for the same background evolution, the large-scale CMB power spectrum can be interpreted in terms of the evolution of the density perturbations for DE and DM.

Neglecting the interaction between dark sectors, for DE with constant EoS $w = -0.9$, we show the CMB power spectrum in Fig. 8(a). Comparing with the ΛCDM model, there is little difference in the CMB at the small l ISW effect. The ISW effect relates to the time variation of the gravitational potentials, which demonstrates little difference between DE with constant EoS and ΛCDM [16]. For DE with constant EoS, the CMB power spectrum keeps the same no matter whether we include the DE fluctuations in the computation or not. The DE fluctuations do not show up in the CMB power spectrum. This is because for DE with a constant EoS, the DE perturbation is negligible. And the result at the large-scale CMB power spectrum agrees with that disclosed in the growth of the DM perturbation in the previous section where the DE fluctuations do not show up for the DE with a constant EoS. Thus, including the DE fluctuations, the CMB power spectrum remains the same as when the perturbations to DE are not taken into account.

For the EDE models, we observed some interesting results in the CMB. We considered both cases where EDE is homogeneous and inhomogeneous in Figs. 9. Besides a slight shift of the position of the acoustic peaks with respect to the ΛCDM model, we see that the CMB power spectrum at small l is different between inhomogeneous and homogeneous EDE. In the homogeneous EDE model in which DE fluctuations are neglected, the small l spectrum is suppressed as compared with that of ΛCDM. In the inhomogeneous EDE model in which DE fluctuations are taken into account, we observe an enhanced power spectrum at low l with respect to ΛCDM. For a given EDE model, the evolutions of background cosmological parameters are the same; the differences in the large-scale CMB power spectrum can be attributed to the evolutions of DE and DM density perturbations. In the last section, we learned that the inhomogeneity in EDE will have an impact

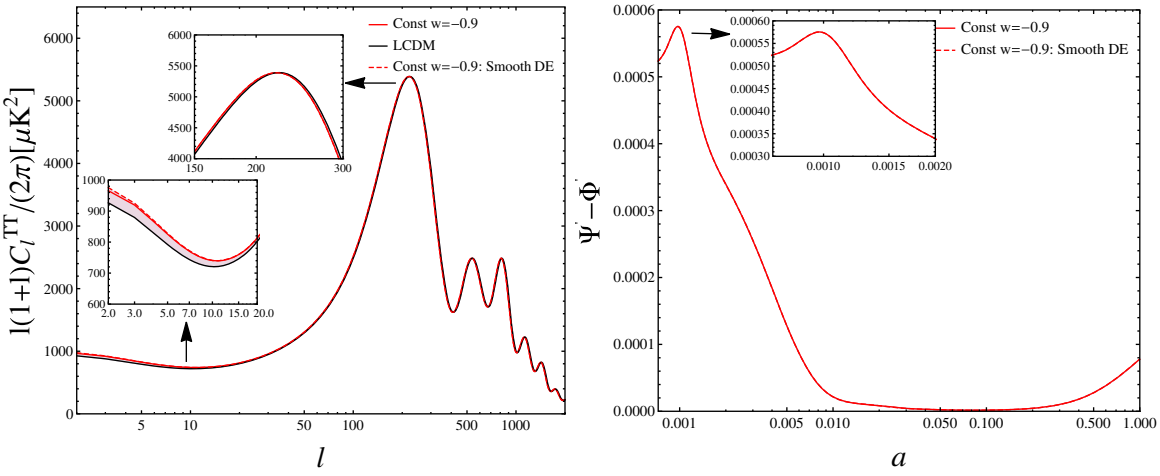

(a) (b)

FIG. 8 (color online). CMB power spectrum and the time derivative of the gravitational potential when the DE EoS is constant, $w = -0.9$.

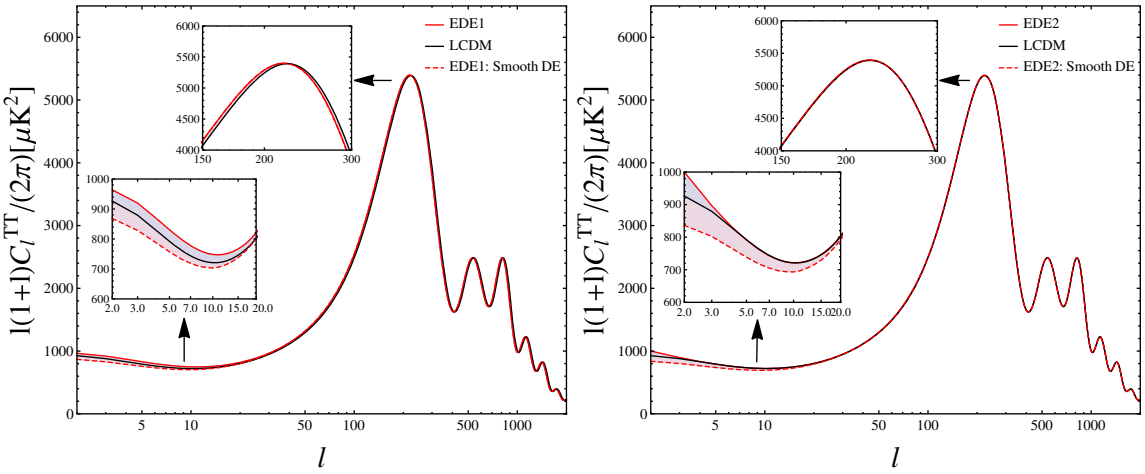

FIG. 9 (color online). CMB power spectrum for EDE models. We compare the CMB power spectrum for the universe with inhomogeneous DE and homogeneous DE. For EDE models, the solid lines refer to inhomogeneous DE, and the dashed lines refer to homogeneous DE.

on the DM perturbations. For the inhomogeneous EDE, the DM perturbation is stronger. The inhomogeneous EDE perturbation also evolves with time. These effects result in a change of the gravitational potential, and the variation of the gravitational potential in time leads to the differences in the ISW effect in the CMB.

Including the interaction between dark sectors, we have a richer physics in the CMB. In the left panel of Fig. 10, we present the CMB power spectrum for the interaction proportional to the energy density of DM. With a positive interaction, we see that the difference at the low l CMB between homogeneous and inhomogeneous EDE is enlarged compared with the zero coupling case. This can be attributed to the enlarged differences in the EDE perturbations together with the DM perturbations between including the EDE fluctuations or not in the presence of the interaction between dark sectors. Besides the difference we observe at low l, at the first peak, the differences between homogeneous and inhomogeneous EDE for the same coupling are small. In the right panel, we show the influence of the interaction proportional to the energy density of DE. With inhomogeneous EDE, the interaction makes the power spectrum higher (the blue solid line) at low l. But with homogeneous EDE, the power spectrum at small l is suppressed (the blue dashed line). The interaction between dark sectors enlarges the differences in the small l

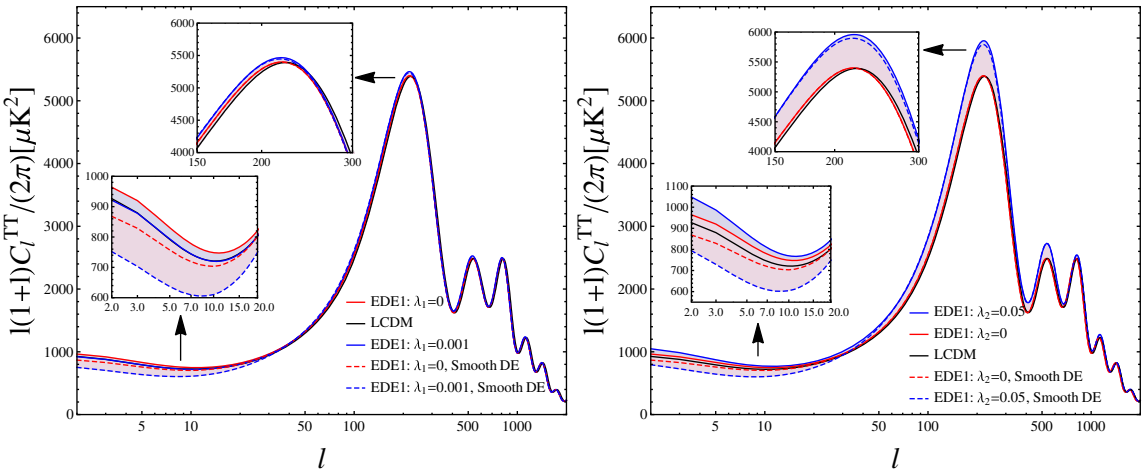

FIG. 10 (color online). CMB power spectrum for EDE coupled to DM. For EDE models, the solid lines refer to inhomogeneous DE, and the dashed lines refer to homogeneous DE.

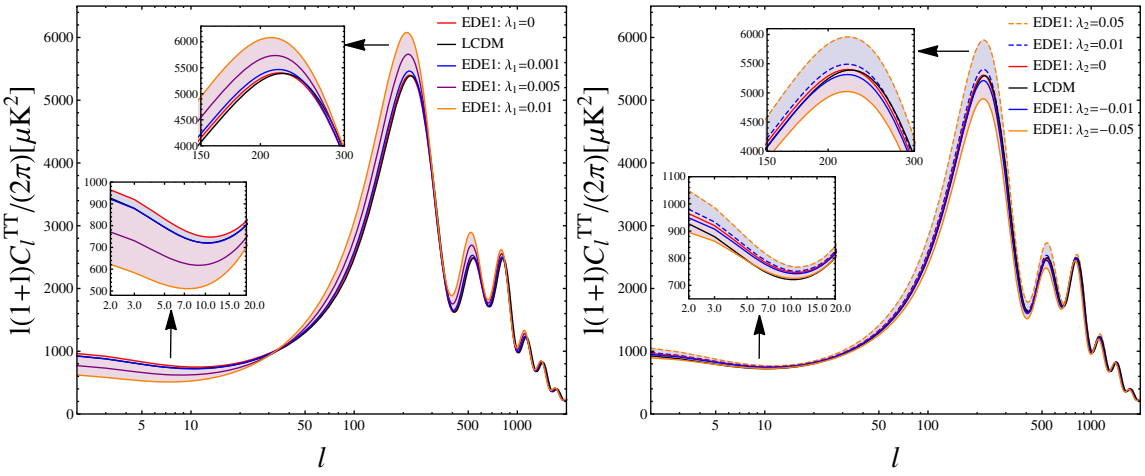

(a) (b)

FIG. 11 (color online). CMB power spectrum for EDE1 coupled to DM. For EDE models, the solid lines refer to inhomogeneous DE, and the dashed lines refer to homogeneous DE.

CMB power spectrum between homogeneous and inhomogeneous EDE. Making the strength of the interaction stronger ($\lambda_2 = 0.05$), we see the clear enhancement of the first peak.

To disclose the influence of different forms and strength of the interaction, we show the CMB power spectrum for EDE1 with various interactions as well as ΛCDM in Fig. 11. We see that when the interaction is proportional to the density of DM, its influence appears not only at small l but also at the first acoustic peak of the CMB power spectrum. A larger λ_1 accommodates the suppression at the low l spectrum but also the enhancement of the first peak. If the interaction is proportional to the energy density of DE, the CMB power spectrum exhibits consistent behaviors both at low l and the first peak: a larger λ_2 leads to the enhancement of the power spectrum. For the EDE models, the influences of the interaction between dark sectors present the same qualitative influence on the CMB as compared with the DE with a constant EoS [23,33].

TABLE I. The priors for cosmological parameters. b(I) refers to the prior of the parameter b of the EDE model for no interaction between DM and DE and the interaction proportional to the energy density of DE. b(II) refers to the prior for the interaction proportional to the energy density of DM.

Parameter	Prior
$\Omega_b h^2$	[0.005, 0.1]
$\Omega_c h^2$	[0.001, 0.5]
100θ	[0.5, 10]
τ	[0.01, 0.8]
n_s	[0.9, 1.1]
$\log(10^{10}A_s)$	[2.7, 4]
w_0	[−0.99, −0.3]
$b(I)$	[0.0, 1]
$b(II)$	[0.1, 1]
λ_1	[0.0, 0.01]
λ_2	[−0.5, 0.5]

IV. FITTING RESULTS

In this section, we fit the EDE models to observations by the Markov chain Monte Carlo (MCMC) method. We modify the public code CosmoMC [34–36] to perform the MCMC analysis. For the EDE models without interaction with DM, we carry out the fittings using two data sets: the CMB observations from Planck(TT + TE + BB + EE) [37–39] and a combined data set of Planck(TT + TE + BB + EE) + BAO [40–42] +SN [43] +H_0 [44]. We try to use these observational data to distinguish between homogeneous and inhomogeneous EDE models. When there is interaction between EDE and DM, we fit the EDE models to the combined data set only, since the CMB data alone cannot constrain the cosmological parameters tightly due to the degeneracy between the coupling strength and DE EoS. In our numerical fittings, the priors of the cosmological parameters are listed in Table I. For the interaction proportional to the energy density of DM, we have to put strict limits on the priors of the parameters. To avoid the negative DE energy density in the early background dynamics and

TABLE II. Best-fit values and 68% C.L. constraints on the inhomogeneous EDE.

	Planck		Planck + BAO + SN + H0	
Parameter	Best fit	68% limits	Best fit	68% limits
w_0	−0.944	$-0.877^{+0.024}_{-0.113}$	−0.989	$-0.975^{+0.002}_{-0.015}$
b	0.111	$0.171^{+0.033}_{-0.171}$	0.012	$0.057^{+0.012}_{-0.057}$
χ^2	9807		10243	

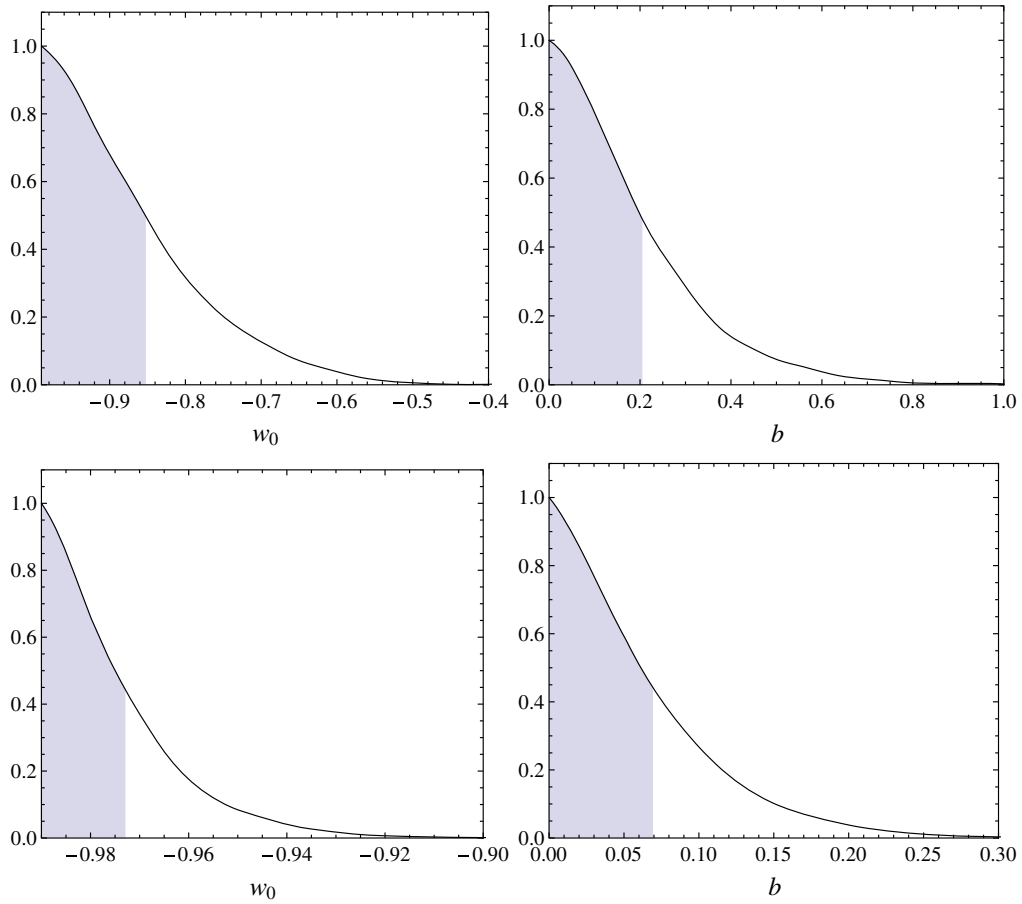

FIG. 12 (color online). Fitting results of the inhomogeneous EDE model. The upper panel is from the Planck data alone, while the lower panel is from the combined data set.

the oscillatory behavior in the time derivative of the gravitational potential, it is necessary that $\lambda_1 > 0$ and $w_0 > -1$, as we discussed above. For the sake of consistency, we set the prior of w_0 bigger than -1 in all models. Besides, b cannot be close to zero if $\lambda_1 > 0$. Otherwise, the DE EoS would be approximately a constant above and close to -1 in the early time of the Universe, as shown in Fig. 1, which is known to cause unstable growth of the

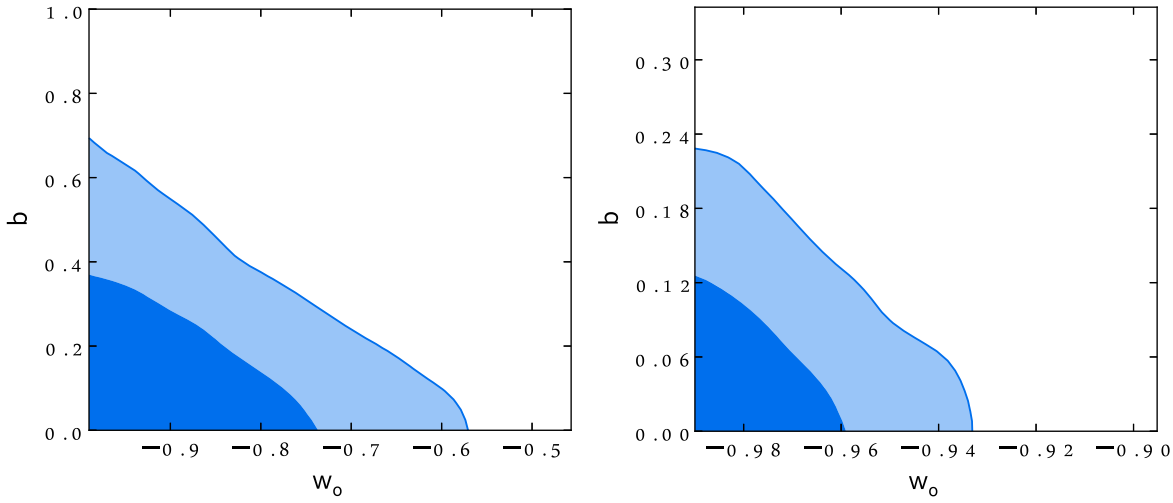

FIG. 13 (color online). Fitting results of the inhomogeneous EDE model in the 2D contour $w_0 - b$. The left panel is from the Planck data alone, while the right panel is from the combined data set.

TABLE III. Best-fit values and 68% C.L. constraints on the homogeneous EDE.

	Planck		Planck + BAO + SN + H0	
Parameter	Best fit	68% limits	Best fit	68% limits
w_0	−0.886	$-0.879^{+0.024}_{-0.111}$	−0.988	$-0.974^{+0.002}_{-0.016}$
b	0.010	$0.173^{+0.034}_{-0.173}$	0.011	$0.061^{+0.013}_{-0.061}$
χ^2	9806		10243	

curvature perturbation [31,45]. Furthermore, considering that the CMB power spectrum is more sensitive to λ_1 than λ_2, following Ref. [21], the prior of λ_1 is tighter than λ_2.

We first assume that DE and DM evolve independently in the MCMC analysis. For the inhomogeneous EDE, with Planck data alone, we show the results in Table II. The likelihood distribution for parameters w_0 and b in the EDE model are shown in the upper panel of Fig. 12. Using the combined data set, we can see how the constraints improve. We list the results in Table II and exhibit the likelihood distributions of w_0 and b in the lower panel of Fig. 12. It is easy to see that the addition of the complementary data clearly improves the constraints on the EDE parameters. This is because the parameters which could be degenerate with the EDE parameters, such as the Hubble parameter, are well constrained by other observations. The 2D contour for $w_0 - b$ is shown in Fig. 13.

We then turn to the case where DE perturbations are neglected. Performing an analysis with Planck data alone, we show the fitting results in Table III and likelihoods for the EDE model parameters in the upper panel of Fig. 14. We find that with Planck data alone, the best fit of w_0 is farther away from −1, and the best fit of b gets smaller than the results of the inhomogeneous case. But the mean values and 68% limits are nearly the same. With combined data sets, the best fit and 68% limit of the inhomogeneous and homogeneous cases show basically no difference. The 2D contour of w_0-b is shown in Fig. 15. Both of them suggest that w_0 is very close to −1 and b is small, which implies a tiny EDE effect.

Considering the interaction between DE and DM, we carry out the MCMC analysis again. We display the likelihood distributions of the EDE parameters and the coupling strength from the combined data sets for inhomogeneous and homogeneous EDE in Figs. 16 and 17,

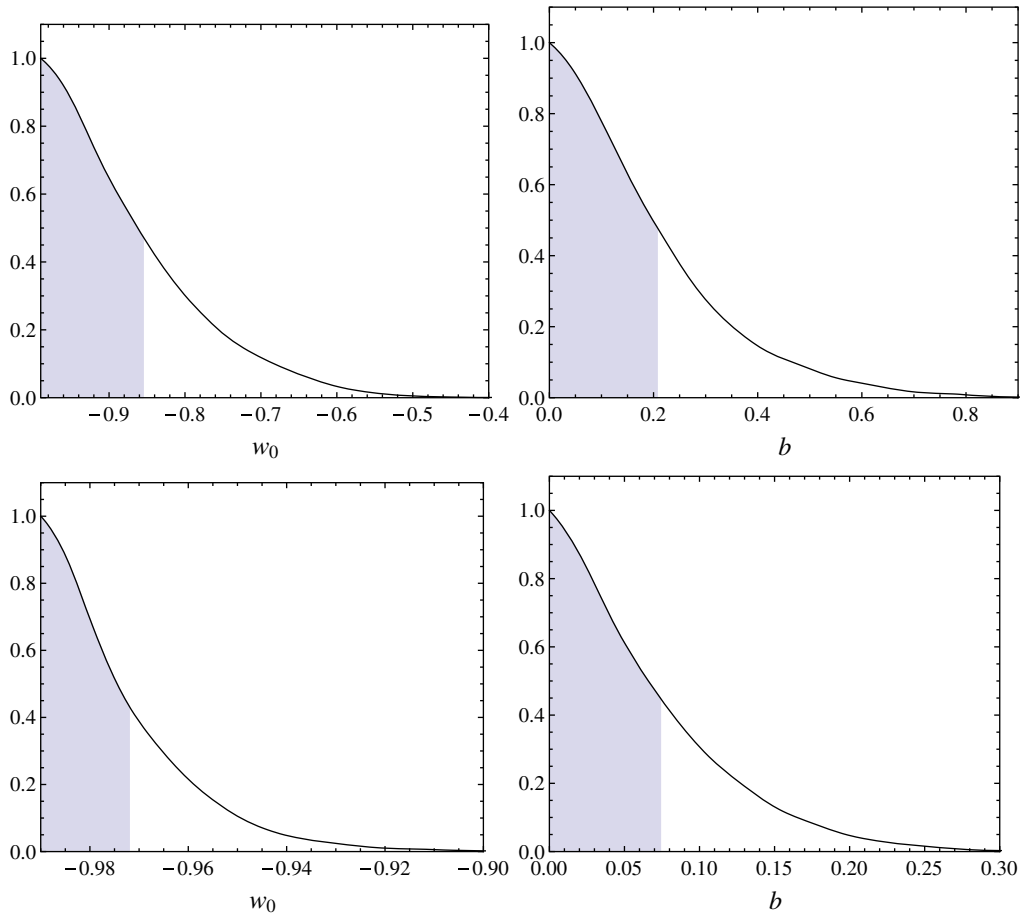

FIG. 14 (color online). Fitting results of the homogeneous EDE model. The upper panel is from the Planck data alone, while the lower panel is from the combined data set.

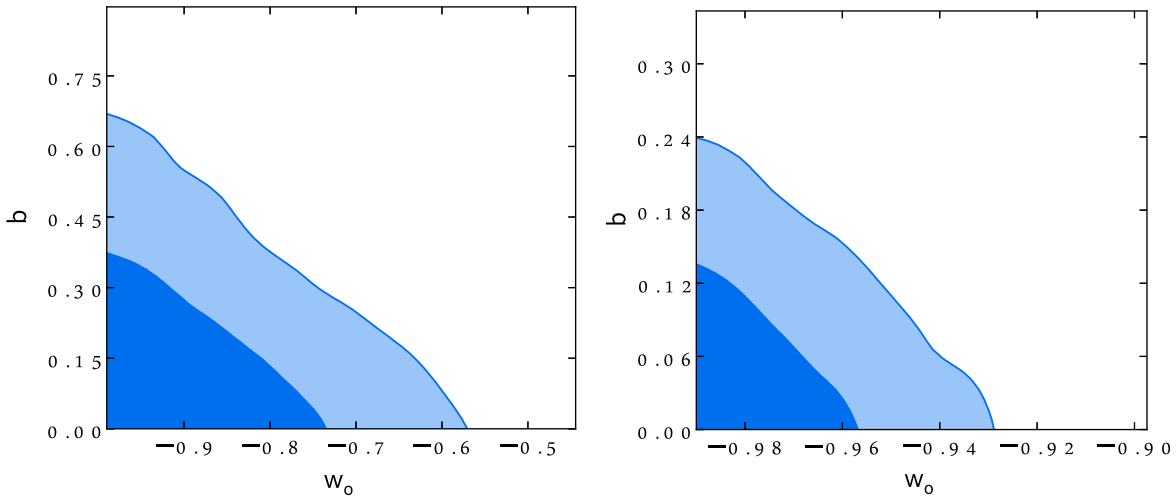

FIG. 15 (color online). Fitting results of the homogeneous EDE model in the 2D contour $w_0 - b$. The left panel is from the Planck data alone, while the right panel is from the combined data set.

respectively. The best-fitting values and 68% limits are listed in Tables IV and V. For inhomogeneous EDE with different forms of interaction, the fitting results of w_0 are similar to that of the noninteracting EDE model. On the other hand, we see that in the presence of interaction, the limit of b is larger, which implies that the EDE effect is stronger. This may be attributed to the choice of prior b(II). But this tendency is also clear when the interaction is proportional to DE density, which shares the same prior of b as noninteracting EDE models.

In the theoretical discussion of the CMB spectrum, we see that the interaction proportional to DM energy density has a stronger impact on the CMB power spectrum than the interaction proportional to the DE energy density. This can be seen also in the fitting results as we find that the limit of λ_1 is much smaller than that of λ_2. The negative best-fit

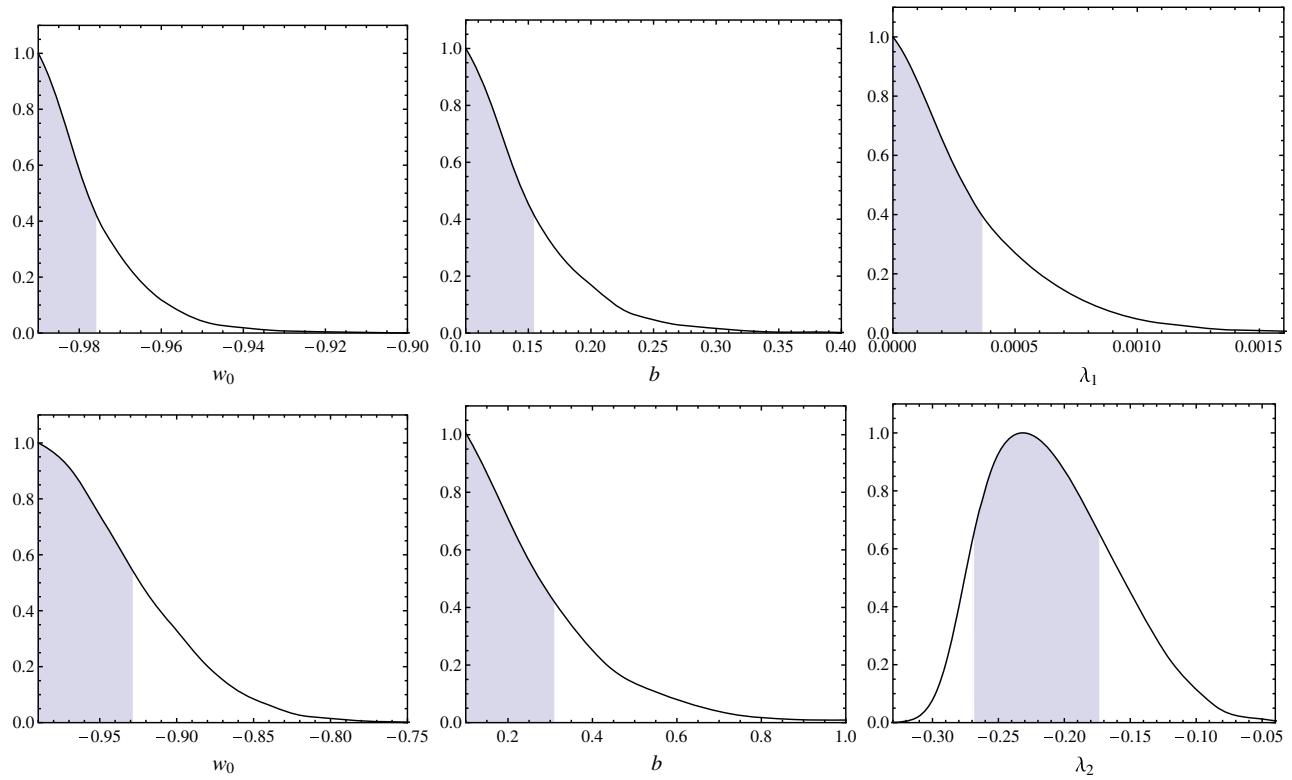

FIG. 16 (color online). Global fitting results of the inhomogeneous EDE model with interaction. The upper panel is for the interaction proportional to the energy density of DM, while the lower panel is for the interaction proportional to the energy density of DE.

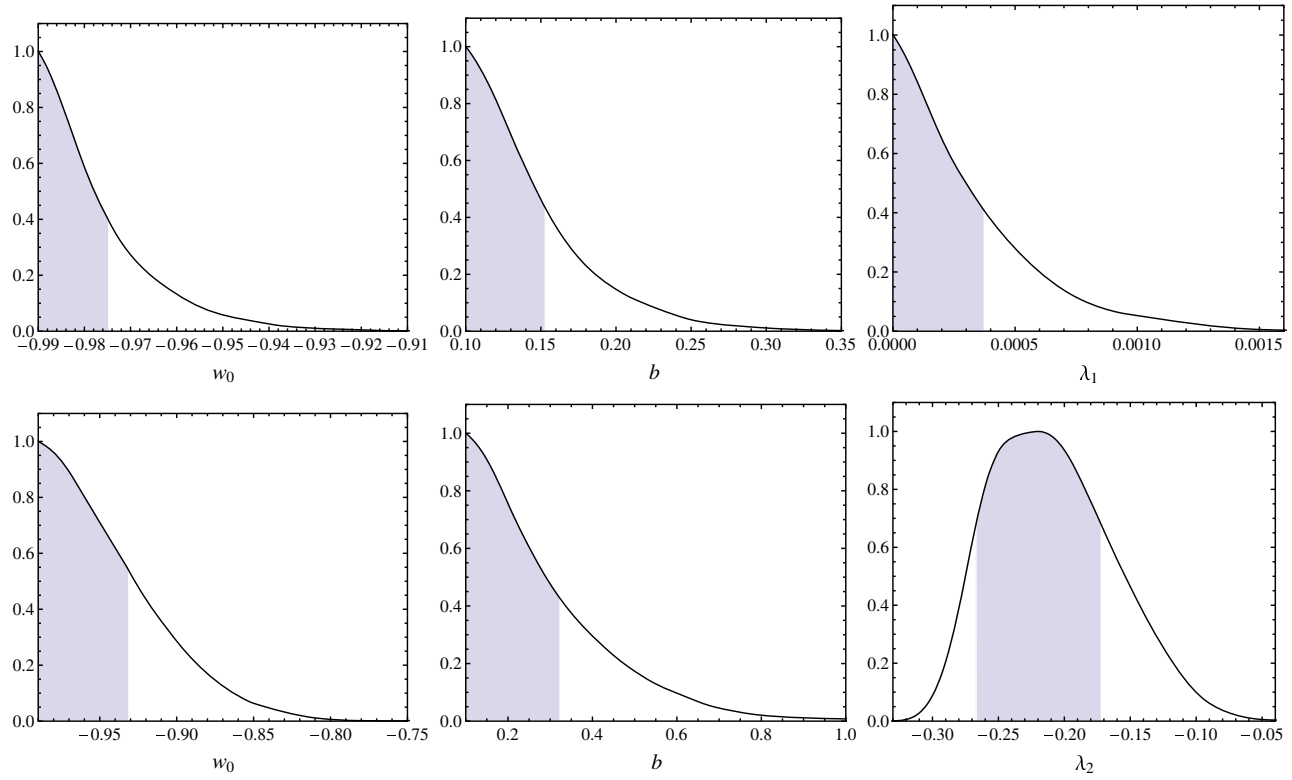

FIG. 17 (color online). Global fitting results of the homogeneous EDE model with interaction. The upper panel is for the interaction proportional to the energy density of DM, while the lower panel is for the interaction proportional to the energy density of DE.

value of λ_2 agrees with the result when the DE EoS is constant [21]. The fitting results for the homogeneous case are similar to the inhomogeneous case.

In the tables of the fitting results, we presented the χ^2 for the best-fit models. When the interaction is proportional to the energy density of DM, the priors of b and λ_1 are highly limited as mentioned above. As a result, the χ^2 is a bit larger than the noninteracting EDE model. On the contrary, the presence of the interaction proportional to DE density decreases the χ^2. Comparing with the ΛCDM model, in which $\chi^2 = 9806, 10242$ for Planck and the combined data set of Planck + BAO + SN + H_0, respectively, we find that the EDE models and their interactions with DM are compatible with current observations.

To examine whether the EDE models allowed by the observations are effective to alleviate the coincidence problem, we plot in Fig. 18 the ratio of the DM energy density to the DE energy density in the best-fit EDE models of the joint analysis and compare them with the ΛCDM prediction. Comparing the EDE models with the ΛCDM model, we find that if the interaction is proportional to the energy density of DM, the ratio evolves more slowly than those in other models. By introducing the interaction between dark sectors, the coincidence problem becomes

TABLE IV. Best-fit values and 68% C.L. constraints on inhomogeneous EDE models with interaction using the combined data set of Planck + BAO + SN + H_0.

	Interaction $\propto \rho_{\rm DM}$		Interaction $\propto \rho_{\rm DE}$	
Parameter	Best fit	68% limits	Best fit	68% limits
w_0	-0.985	$-0.978^{+0.002}_{-0.012}$	-0.989	$-0.941^{+0.012}_{-0.049}$
b	0.113	$0.147^{+0.007}_{-0.047}$	0.200	$0.274^{+0.034}_{-0.174}$
λ_1	0.000274	$0.000309^{+0.000054}_{-0.000309}$	⋯	⋯
λ_2	⋯	⋯	-0.137	$-0.209^{+0.035}_{-0.050}$
χ^2	10247		10238	

TABLE V. Best-fit values and 68% C.L. constraints on homogeneous models with interaction using the combined data set of Planck + BAO + SN + H_0.

	Interaction $\sim\rho_{\rm DM}$		Interaction $\sim\rho_{\rm DE}$	
Parameter	Best fit	68% limits	Best fit	68% limits
w_0	-0.974	$-0.977^{+0.002}_{-0.013}$	-0.966	$-0.943^{+0.011}_{-0.047}$
b	0.115	$0.144^{+0.008}_{-0.044}$	0.123	$0.282^{+0.038}_{-0.182}$
λ_1	0.000109	$0.000311^{+0.000057}_{-0.000311}$	⋯	⋯
λ_2	⋯	⋯	-0.189	$-0.209^{+0.036}_{-0.058}$
χ^2	10248		10237	

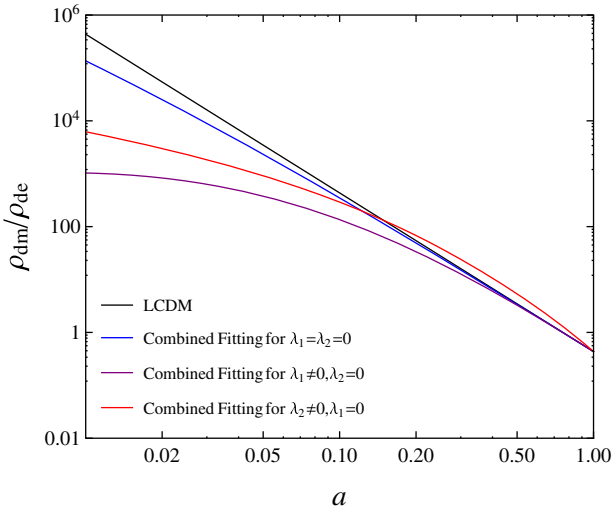

FIG. 18 (color online). Ratio of DM energy density to DE energy density of the best-fit EDE models.

less acute. We conclude that the EDE model is compatible with observations and it is effective to alleviate the coincidence problem.

V. CONCLUSIONS AND DISCUSSIONS

In this paper, we have studied the influence of EDE on DM perturbations. We have observed that, different from DE models with a constant EoS, DM perturbation is larger in inhomogeneous EDE models than in the homogeneous EDE model in which DE fluctuation is neglected. We have also disclosed the difference between inhomogeneous and homogeneous EDE in the large-scale CMB power spectrum. It is expected that the probe of the growth of the large-scale structure and small l CMB power spectrum can help to distinguish homogeneous and inhomogeneous EDE models.

Furthermore, we have extended our discussion to the interaction between EDE and DM. We have observed that an interaction between EDE and DM also affects DM perturbations and the small l CMB power spectrum, which may be degenerate with the effect of DE fluctuations. Comparing these effects, we found that the interaction between EDE and DM has a stronger influence on DM perturbations and on the ISW effect.

We have constrained the EDE models using Planck data and a combined data set of Planck + BAO + SN + H_0. The analysis showed that the coincidence problem in all best-fit EDE models is less severe than in the ΛCDM model. The positive coupling between EDE and DM proportional to the energy density of DM is particularly effective to alleviate the coincidence problem. It can be clearly seen in Fig. 18 that with the positive coupling between EDE and DM proportional to the energy density of DM, it has a longer period for the DE and DM to be comparable.

It is interesting to further examine whether the disclosed impacts of the DE fluctuations and the interaction between DE and DM on observables are specific to EDE models. A lot of efforts on this problem are called for.

ACKNOWLEDGMENTS

We acknowledge financial support from National Basic Research Program of China (973 Program No. 2013CB834900) and National Natural Science Foundation of China. E. A. acknowledges financial support from Conselho Nacional de Desenvolvimento Científico e Tecnológico and from Fundação de Amparo à Pesquisa do Estado de São Paulo.

[1] S. Weinberg, Rev. Mod. Phys. **61**, 1 (1989).
[2] L. P. Chimento, A. S. Jakubi, D. Pavon, and W. Zimdahl, Phys. Rev. D **67**, 083513 (2003).
[3] A. Hojjati, E. V. Linder, and J. Samsing, Phys. Rev. Lett. **111**, 041301 (2013).
[4] M. Doran, M. Lilley, J. Schwindt, and C. Wetterich, Astrophys. J. **559**, 501 (2001).
[5] U. Alam, Astrophys. J. **714**, 1460 (2010).
[6] M. Doran, K. Karwan, and C. Wetterich, J. Cosmol. Astropart. Phys. 11 (2005) 007.
[7] P. Wu and H. Yu, Phys. Lett. B **643**, 315 (2006).
[8] J. Bielefeld, W. L. Kimmy Wu, R. R. Caldwell, and O. Dore, Phys. Rev. D **88**, 103004 (2013).
[9] J. Q Xia and M. Viel, J. Cosmol. Astropart. Phys. 04 (2009) 002.
[10] C. M. Müller, G. Schäfer, and C. Wetterich, Phys. Rev. D **70**, 083504 (2004).
[11] M. Bartelmann, M. Doran, and C. Wetterich, Astron. Astrophys. **454**, 27 (2006).
[12] U. Alam, Z. Lukic, and S. Bhattacharya, Astrophys. J. **727**, 87 (2011).
[13] F. Fontanot, V. Springel, R. E. Angulo, and B. Henriques, Mon. Not. R. Astron. Soc. **426**, 2335 (2012).
[14] M. Grossi and V. Springel, Mon. Not. R. Astron. Soc. **394**, 1559 (2009).
[15] R. C. Batista and F. Pace, J. Cosmol. Astropart. Phys. 06 (2013) 044.
[16] S. Das, A. Shafieloo, and T. Souradeep, J. Cosmol. Astropart. Phys. 10 (2013) 016.
[17] M. Baldi, Mon. Not. R. Astron. Soc. **422**, 1028 (2012).

[18] C. Wetterich, Phys. Lett. B **594**, 17 (2004).
[19] M. Sadegh Movahed and S. Rahvar, Phys. Rev. D **73**, 083518 (2006).
[20] Y. G. Gong, Classical Quantum Gravity **22**, 2121 (2005).
[21] A. A. Costa, X. D. Xu, B. Wang, E. G. M. Ferreira, and E. Abdalla, Phys. Rev. D **89**, 103531 (2014).
[22] X. D. Xu, B. Wang, P. J. Zhang, and F. Atrio-Barandela, J. Cosmol. Astropart. Phys. 12 (2013) 001.
[23] J. H. He, B. Wang, and E. Abdalla, Phys. Rev. D **83**, 063515 (2011).
[24] J. H. He, B. Wang, E. Abdalla, and D. Pavon, J. Cosmol. Astropart. Phys. 12 (2010) 022.
[25] E. Abdalla, L. R. Abramo, L. Sodre, and B. Wang, Phys. Lett. B **673**, 107 (2009).
[26] E. Abdalla, L. Graef, and B. Wang, Phys. Lett. B **726**, 786 (2013).
[27] S. Micheletti, E. Abdalla, and B Wang, Phys. Rev. D **79**, 123506 (2009).
[28] S. Micheletti, J. Cosmol. Astropart. Phys. 05 (2010) 009.
[29] O. Bertolami, P. Carrilho, and J. Paramos, Phys. Rev. D **86**, 103522 (2012).
[30] E. Abdalla, E. G. M. Ferreira, J. Quintin, and B. Wang, arXiv:1412.2777.
[31] J. H. He, B. Wang, and E. Abdalla, Phys. Lett. B **671**, 139 (2009).
[32] J. H. He, B. Wang, and Y. P. Jing, J. Cosmol. Astropart. Phys. 07 (2009) 030.
[33] J. H. He, B. Wang, and P. J. Zhang, Phys. Rev. D **80**, 063530 (2009).
[34] A. Lewis and S. Bridle, Phys. Rev. D **66**, 103511 (2002).
[35] A. Lewis, Phys. Rev. D **87**, 103529 (2013).
[36] A. Lewis, A. Challinor, and A. Lasenby, Astrophys. J. **538**, 473 (2000).
[37] Planck Collaboration, Astron. Astrophys. **571**, A1 (2014).
[38] Planck Collaboration, Astron. Astrophys. **571**, A16 (2014).
[39] Planck Collaboration, Astron. Astrophys. **571**, A15 (2014).
[40] F. Beutler, C. Blake, M. Colless, D. H. Jones, L. Staveley-Smith, L. Campbell, Q. Parker, W. Saunders, and F. Watson, Mon. Not. R. Astron. Soc. **416**, 3017 (2011).
[41] N. Padmanabhan, X. Xu, D. J. Eisenstein, R. Scalzo, A. J. Cuesta, K. T. Mehta, and E. Kazin, Mon. Not. R. Astron. Soc. **427**, 2132 (2012).
[42] L. Anderson *et al.*, Mon. Not. R. Astron. Soc. **427**, 3435 (2012).
[43] N. Suzuki *et al.*, Astrophys. J. **746**, 85 (2012).
[44] A. G. Riess, L. Macri, S. Casertano, H. Lampeitl, H. C. Ferguson, A. V. Filippenko, S. W. Jha, W. Li, and R. Chornock, Astrophys. J. **730**, 119 (2011).
[45] X. D. Xu, J. H. He, and B. Wang, Phys. Lett. B **701**, 513 (2011).